

AD-A148 656

VOLTAMMETRY AND COULOMETRY WITH IMMERSSED THIN LAYER
ELECTRODES PART 2 PRA. (U) UTAH UNIV SALT LAKE CITY
DEPT OF CHEMISTRY A S HINMAN ET AL. 28 NOV 84 TR-31
N00014-83-K-0470

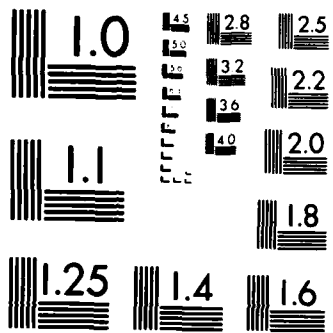
1/1

UNCLASSIFIED

F/G 7/4

NL





MICROCOPY RESOLUTION TEST CHART
NATIONAL BUREAU OF STANDARDS-1963-A

12

AD-A148 656

OFFICE OF NAVAL RESEARCH
Contract N00014-83-K-0470
Task No. NR 359-718
TECHNICAL REPORT NO. 31

Voltammetry and Coulometry with Immersed Thin Layer
Electrodes. Part II. Practical Considerations and
Experimental Results.

By

A. Scott Hinman
Stanley Pons
John Cassidy

Prepared for Publication in

Electrochim. Acta

University of Utah
Department of Chemistry
Salt Lake City, Utah 84112

November 28, 1984

SDTIC
ELECTE
DEC 21 1984
E

Reproduction in whole or in part is permitted for
any purpose of the United States Government

This document has been approved for public release
and sale; its distribution is unlimited.

84 12 12 040

U116 FILE WEL

REPORT DOCUMENTATION PAGE		READ INSTRUCTIONS BEFORE COMPLETING FORM
1. REPORT NUMBER 31	2. GOVT ACCESSION NO. AD A148658	3. RECIPIENT'S CATALOG NUMBER
4. TITLE (and Subtitle) Voltammetry and Coulometry with Immersed Thin Layer Electrodes. Part II. Practical Considerations and Experimental Results		5. TYPE OF REPORT & PERIOD COVERED Technical Report # 31
7. AUTHOR(s) A. Scott Hinman; Stanley Pons*; John Cassidy		6. PERFORMING ORG. REPORT NUMBER
5. PERFORMING ORGANIZATION NAME AND ADDRESS University of Utah Department of Chemistry Salt Lake City, UT 84112		8. CONTRACT OR GRANT NUMBER(s) N00014-83-K-0470
11. CONTROLLING OFFICE NAME AND ADDRESS Office of Naval Research Chemistry Program - Chemistry Code 472 Arlington, Virginia 22217		10. PROGRAM ELEMENT, PROJECT, TASK AREA & WORK UNIT NUMBERS Task No. NR 359-718
14. MONITORING AGENCY NAME & ADDRESS (if different from Controlling Office)		12. REPORT DATE November 28, 1984
		13. NUMBER OF PAGES 13
		15. SECURITY CLASS. (of this report) Unclassified
		15a. DECLASSIFICATION/DOWNGRADING SCHEDULE
16. DISTRIBUTION STATEMENT (of this Report) This document has been approved for public release and sale; its distribution unlimited.		
17. DISTRIBUTION STATEMENT (of the abstract entered in Block 20, if different from Report)		
18. SUPPLEMENTARY NOTES		
19. KEY WORDS (Continue on reverse side if necessary and identify by block number) Thin layer electrochemistry, voltammetry		
20. ABSTRACT (Continue on reverse side if necessary and identify by block number) We have shown that geometrical considerations in the design of immersed thin layer electrochemical (ITLE) cells are important in the satisfactory performance of voltammetric experiments in solutions of high specific resistivity. In this paper, practical cell design and experimental results for a variety of systems are considered.		

Voltammetry and Coulometry with Immersed
Thin Layer Electrodes. Part II. Practical
Considerations and Experimental Results

A. Scott Hinman
Department of Chemistry
University of Calgary
Calgary, Alberta
CANADA

Stanley Pons* and John Cassidy
Department of Chemistry
University of Utah
Salt Lake City, UT 84112

*To whom all correspondence should be addressed.

Accession For	
NTIS GRA&I	<input checked="" type="checkbox"/>
IEEE Xplore	<input type="checkbox"/>
Unannounced	<input type="checkbox"/>
Justification	
Exempt from	
Classification/	
Availability Codes	
and/or	
Distribution Statement	
A-1	



INTRODUCTION

We have shown (1) that geometrical considerations in the design of immersed thin layer electrochemical (ITLE) cells are important in the satisfactory performance of voltammetric experiments in solutions of high specific resistivity (1). In this paper, practical cell design and experimental results for a variety of systems are considered.

EXPERIMENTAL

Chemicals. Tetra n-butylammonium perchlorate (TBAP) (Southwest Analytical) was used as received after drying in vacuo at 40°C. 1-2 dichloroethane was extracted with an equal volume of cold concentrated sulphuric acid followed by extraction with 10 volumes of 5% NaOH. The product was dried over anhydrous sodium sulfate, distilled from calcium hydride, and stored in the dark. Immediately prior to use, the dichloroethane was passed down a basic alumina column (Woelm B super 1). HPLC grade acetonitrile (Caledon) was passed through an alumina column (Woelm N super 1) before use. Water was triply distilled.

Tetraphenylporphinatozinc (II) (Zn(II)TPP) was prepared according to Alder et.al. (2) from tetraphenylporphine (Aldrich) and zinc acetate. The product was purified chromatographically on an alumina column using chloroform as eluent. All other chemicals were reagent grade and used without further purification.

CELL DESIGN

A thin layer cell was constructed using the radial concentric configuration, and its performance evaluated in a variety of solvent-electrolyte systems. Two electrodes were tested. The first consisted of a

planar glassy carbon disc, ca 3 mm in diameter, sealed with epoxy into a glass tube. The second consisted of a 1.5 mm diameter Pt wire press fitted into the end of a Teflon tube such that the tip of the wire was flush with the lower surface of the tube. The wire was offset in the tube, allowing for closer proximity of the Luggin tip and the edge of the working electrode. The experimental arrangement, including a detail of the offset platinum button electrode, is illustrated in Figure 1. The secondary electrode used was a platinum wire formed into a circle concentric with the working electrode circumference.

Both (the Carbon and Pt working) electrodes were machined flush to the lower surface of the Teflon mounting block by inserting the electrode into the block, tightening the securing screw, and working the lower surface of the assembly across a piece of 600 grit wet and dry sandpaper placed on top of a piece of heavy plate glass. This was followed by polishing the 0.05 μm alumina on a soft polishing felt, mounted on plate glass, until the working electrode exhibited a mirror-like finish.

The Teflon mount and electrode assembly was positioned above the surface of a microscope slide by means of two glass spacers cut from a second glass slide. The spacers and slide were fixed to the bottom of the Teflon mount with the aid of two laboratory pinch clamps. A piece of glassine powder paper (Eli Lilly) was then placed between the surface of the microscope slide and the working electrode, and the electrode was then pushed, as firmly as possible without breaking the glass, into it. After tightening the securing screw, the powder paper could be pulled out of the thin layer cavity, providing adequate polishing of the working electrode surface had been accomplished. The entire assembly was then lowered into a beaker containing the solution of interest. In order to exclude contamination by O_2 or H_2O ,

experiments were carried out in a polyethylene glove bag flushed with dry argon. A glass cover was placed over the beaker in order to help prevent solution losses from evaporation.

The thickness of the thin layer cavity was found to vary between 5 and 15 μm , as calculated on the basis of the charge required to completely electrolyze a known quantity of material within the cavity. Once a suitable thin layer thickness was attained ($<10 \mu\text{m}$ to minimize diffusion into the cavity), the assembly could be used repetitively provided repositioning of the working electrode had not occurred. Rinsing of the electrode cavity was achieved by directing a rapid stream of fresh solution at the edge of the working electrode from the tip of a disposable pipet inserted into the Luggin locator notch. Ten such rinsings were found to always produce reproducible results.

A Hi-Tek model DT2101 potentiostat was used in conjunction with a Hi-Tek model PPR1 waveform generator to control the working electrode potential with respect to an aqueous saturated calomel electrode constructed in this laboratory. Because the level of the currents measured was exceptionally small, a Bentham model 210 E current follower capable of measuring currents in the pA to μA range was used instead of the current follower incorporated into the potentiostat. A 100 pF capacitor shunting the secondary and reference electrodes was included in the experimental hook-up. This improved the noise and stability characteristics of the system. The use of such stabilizing capacitors has been discussed (3). In coulometric experiments, a low input current precision operational-amplifier based integrator constructed in this laboratory was used to monitor the charge passed. Positive feedback compensation of solution resistance was not employed in any of the experiments.

VOLTAMMETRIC EXPERIMENTAL RESULTS

Figure 2a presents a cyclic voltammogram obtained in 1.0 M aqueous KCl containing 1.0 mM $K_4Fe(CN)_6$ at the glassy carbon thin layer electrode. The small difference in the anodic and cathodic peak potentials, $\Delta E_p = 30$ mV, corresponds to near-ideal thin layer behavior for a reversible system, and the width of the forward peak at half-height is 105 mV in good agreement with the 90 mV prediction of eqn. [4] of (1) for a reversible one-electron process. The formal potential of the redox couple was estimated as the average of the forward and reverse peak potentials, and is identical to the value of 0.219 volts vs SCE obtained for the half-wave potential by conventional cyclic voltammetry under the same conditions.

Figure 2b illustrates the charge passed as a function of potential as recorded during the anodic sweep of Figure 2a. Potential scanning coulometry at thin layer electrodes has been used previously (4), but the method of defining the endpoint was not discussed. In general, three essentially linear regions are observed in the coulometric wave. The slowly rising region at the foot of the wave is due to integration of the residual charging current, while that at potentials well past the formal potential of the redox couple represents, to a large extent, the diffusion of electroactive species into the thin layer cavity from the bulk solution. The rapidly rising portion in between the two extremes is due to the electrolysis of the electroactive species trapped within the thin layer next to the working electrode. The charge corresponding to complete electrolysis of the analyte has been taken as that lying between the points A and B in Figure 2b as obtained by the indicated linear extrapolations. We have found that use of this method to estimate electrolysis endpoints leads to linear plots of charge vs. concentration with the intercept at the origin (wide infra). The precision

attainable is often better than $\pm 3\%$ relative standard deviation. This is in excess of that generally required for n -value determinations.

While the glassy carbon electrode is apparently adequate for use in aqueous systems, its performance in non-aqueous systems was not deemed satisfactory. For the oxidation of Zn(II)TPP, in dichloroethane solutions, the forward and reverse peaks were separated in excess of 250 mV even when very low sweep rates were used, and resolution between successive electron transfer steps was not as complete as had been hoped. For these reasons, the platinum thin layer electrode, as already described, was constructed on the basis of predictions that the smaller electrode radius would improve the performance of the thin layer cell.

Figure 3 illustrates thin layer cyclic voltammograms at the platinum electrode obtained for 1 mM ferrocene in $\text{CH}_3\text{CN}/0.1 \text{ M TBAP}$ at potential sweep rates of 10, 100, and 200 $\text{mV}\cdot\text{s}^{-1}$. At potential sweep rates of 10 $\text{mV}\cdot\text{s}^{-1}$ or less, the forward and reverse peaks are separated by less than 50 mV. At a sweep rate of 100 $\text{mV}\cdot\text{s}^{-1}$, the peaks are separated by 120 mV, while at 200 $\text{mV}\cdot\text{s}^{-1}$, a 210 mV peak separation is observed. These latter sweep rates are far in excess of those commonly used. The ability to vary the sweep rate is an important consideration in work where qualitative mechanistic diagnosis of electrode reactions is sought, and is responsible to a large extent for the popularity of conventional cyclic voltammetry. In at least some cases, thin layer techniques should be even more powerful in this regard. Some indication of this has appeared in the literature (5-7).

It will be noticed, with reference to Figure 3, that the voltammograms obtained at higher sweep rates, although exhibiting a greater degree of asymmetry, are in fact better defined against the background. This is due to the fact that currents associated with diffusion from the solution bulk are

independent of potential scan rate, while the peak currents increase with scan rate, as indicated by eqn. [1] of (1). The greater influence of bulk diffusion at electrodes of smaller radius, as predicted, is manifested in the increased current observed at potentials past the forward peak in the lower sweep rate voltammograms.

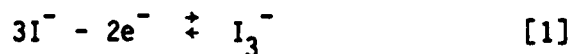
Figure 4 illustrates the thin layer cyclic voltammetric behavior of Zn(II)TPP in $C_2H_4Cl_2/0.2$ M TBAP at anodic potentials. The two successive anodic waves correspond to formation of the cation radical and dication, respectively, while the cathodic waves are due to reduction of these species. At low sweep rates near ideal behavior is observed for this system. At $3\text{ mV}\cdot\text{s}^{-1}$ forward and reverse peaks for the individual redox processes are separated by 30 mV and the peak widths at half-height are 110 mV. Even at sweep rates as high as $100\text{ mV}\cdot\text{s}^{-1}$ successive redox processes are completely resolved.

Figure 5 presents charge versus potential plots recorded during anodic sweeps for this system. The coulometric waves were recorded at various sweep rates and have been successively displaced by 200 mV in the Figure for purposes of clarity. It is evident that the waves become much better defined as the sweep rate is increased, and the electrolysis endpoints are therefore more easily determined.

Figure 6 illustrates the apparent charge required for complete electrolysis in the first anodic wave plotted as a function of potential sweep rate. The endpoints were determined by the method previously outlined in Figure 2b. At lower sweep rates there is a trend to higher values. This can be ascribed to the longer time period available for diffusion of reactant into the thin layer cavity during the course of the experiment. At sweep rates greater than $20\text{ mV}\cdot\text{s}^{-1}$, a constant value is obtained, and higher sweep rates

are therefore recommended for coulometric work.

Figure 7 illustrates the thin layer cyclic voltammetric behavior observed at the platinum electrode for the oxidation of tetra-n-butylammonium iodide in $\text{CH}_3\text{CN}/0.1 \text{ M TBAP}$. The successive anodic waves correspond to the oxidation of I^- and I_3^- , respectively, while the cathodic waves represent the reduction of I_2 and I_3^- . The pertinent equilibria, as indicated by Popov and Geske (8), are:



and

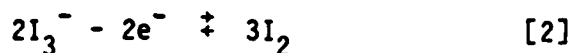


Figure 8 is a plot of the charge required for complete conversion of the I^- within the cavity to I_3^- , as determined by the methods described here. The linearity of the plot and the zero intercept serve to demonstrate the validity of the method. All points lie within $\pm 5\%$ (vertically) of the indicated line.

The ratio of the charge associated with the second oxidation in Figure 7 to that for the first was determined as 0.50 when the sweep rate was 25 mV/s. This is in agreement with the value expected from the stoichiometry of reactions [1] and [2]. We emphasize the applicability of thin layer voltammetry to rapid and accurate determination of the stoichiometry of complex electrode reactions.

CHRONOCOULOMETRIC RESULTS

In conventional voltammetric cells, when the electrode potential is suddenly pulsed to a value where a faradaic electron transfer process occurs at a diffusion controlled rate, the charge vs. time behavior (9) at later times is given by:

$$Q = \frac{2nFAD^{1/2}C^*t^{1/2}}{\pi^{1/2}} + Q_{DL} \quad [3]$$

where Q is the total charge passed, D is the diffusion coefficient of the electroactive species and C^* is its bulk concentration. Q_{DL} is the charge associated with charging of the double layer and A is the electrode area.

If the same experiment is carried out at an immersed thin layer electrode, the charge recorded at times after that corresponding to complete electrolysis of the species within the thin layer cavity will be dictated solely by diffusion into the cavity. By analogy to equation [3] the charge-time transient obtained at later times should follow an equation of the form

$$Q = \frac{2nFA'D^{1/2}C^*t^{1/2}}{\pi^{1/2}} + Q' \quad [4]$$

where A' is the exposed surface area of the cylinder contained between the working electrode surface and the glass insulator, and Q' is a constant dictated by the length of time required for complete electrolysis of the species within the thin layer cavity. A plot of Q vs $t^{1/2}$ should therefore exhibit a linear region at later times. The line should be displaced along the Q axis by some amount allowing the determination of n and A' , and its

slope should then allow the determination of D. The parameters n and D should therefore be available from a single experiment. In most other voltammetric techniques, cyclic voltammetry and chronoamperometry, for instance, only the product $nD^{1/2}$, or $n^{3/2} D^{1/2}$, is available.

Figure 9 presents a Q vs $t^{1/2}$ plot obtained for the one-electron oxidation of $(ClO_4)Mn(III)TPP$ in $C_2H_4Cl_2/0.2 M TBAP$ at the platinum thin layer electrode. The background charge was obtained in a separate experiment in the absence of electroactive species and was subtracted from the data. The predicted linear behaviour is indeed observed at later times. The charge indicated at point A in the figure is 4% less than that indicated by potential scanning coulometry as corresponding to complete electrolysis of the species within the thin layer cavity. Experimental evaluation of the applicability of the proposed method to the simultaneous determination of n-values and diffusion coefficients has been reserved for a later project.

In summary, we feel that reasonable care in the design of thin layer cells leads to the quantitative use of voltammetry and coulometry in systems with high specific resistivities. In the end, the effort is not much more than that required for conventional cyclic voltammetry, whereas the advantages of analysis using thin layer techniques are greater than those in conventional voltammetry.

ACKNOWLEDGEMENTS

The author thanks the Office of Naval Research for support of part of this work. One of us (A.S.H.) thanks the Alberta Heritage Foundation for Medical Research for financial support.

REFERENCES

1. A. Scott Hinman, Stanley Pons, and John Cassidy, (Part I).
2. A.D. Adler, F.R. Longo, F. Kampas, and J. Kim, J. Inorg. Nucl. Chem. 32, 2443 (1970).
3. D.T. Sawyer and J.L. Roberts, Jr., "Experimental Electrochemistry for Chemists", Wiley Interscience, New York, 1974.
4. D.M. Oglesby, L.B. Anderson, B.McDuffy, and C.N. Reilly, Anal. Chem. 37, 1317 (1965).
5. M. Fleischmann, D. Pletcher, and A. Rafinski, J. Electroanal. Chem. 38, 323 (1972).
6. Ibid. p. 329.
7. E. Laveron, ibid 87, 31 (1978).
8. A.I. Popov and D.H. Geske, J. Amer. Chem. Soc. 80, 1340 (1958).
9. F.C. Anson, Anal. Chem. 38, 54 (1966).

FIGURE LEGENDS

Figure 1. Details of thin layer electrode assembly.

Figure 2. (a) Cyclic voltammogram of 1 mM $K_4Fe(CN)_6$ at glassy carbon thin layer electrode in 1 M aq. KCl, $v = 5 \text{ mV-s}^{-1}$. (b) Charge vs potential recorded during forward sweep of voltammogram in (a).

Figure 3. Cyclic voltammograms of 1 mM ferrocene at Pt thin layer electrode in $CH_3CN(0.1 \text{ M TBAP})$.

Figure 4. Cyclic voltammograms of 1 mM $Zn(II)TPP$ at Pt electrode in $C_2H_4Cl_2(0.2 \text{ M TBAP})$. Upper curve, $v = 100 \text{ mV-s}^{-1}$; lower curve, $v = 5 \text{ mV-s}^{-1}$.

Figure 5. Potential scanning coulometry for 1 mM Zn(II)TPP at Pt thin layer electrode in $C_2H_4Cl_2$ (0.2 M TBAP) as recorded at various sweep rates.

Figure 6. Apparent charge required for complete 1-electron oxidation of 1 mM Zn(II)TPP in $C_2H_4Cl_2$ (0.2 M TBAP) as determined by potential scanning coulometry at Pt thin layer electrode at various sweep rates.

Figure 7. Cyclic voltammogram of 2 mM I^- in CH_3CN (0.1 TBAP) at Pt thin layer electrode.

Figure 8. Charge vs concentration for first oxidation of I^- in CH_3CN (0.1 M TBAP) as determined by potential scanning coulometry at Pt thin layer electrode.

Figure 9. Charge vs $t^{1/2}$ for 1-electron oxidation of $(\text{ClO}_4)\text{Mn}(\text{III})\text{TPP}$ in $\text{C}_2\text{H}_4\text{Cl}_2$ (0.2 M TBAP) at Pt thin layer electrode under potential step conditions.

END

FILMED

1-85

DTIC